Final Report:
"Generalized Double-Slot Waveguide Components for Millimeter-Wave Integrated Circuits"

1. Introduction.

1.1 Creation of effective and cheap Superfast Information Processing Systems (SIPSs) processing in EHF band directly is not possible without utilization of Three-Dimensional Integrated Circuits (TDICs) [1-3]. This tendency of up-to-date radio engineering and computer technology is alternative for processors with integrated circuit (IC) which are built with planar technology and working on relatively low frequencies (about some hundreds of MHz).

Main advantages of TDIC are strong dimensional decrease (about 1-3 orders) with compare to conventional planar IC technology. It allows every layer of TDIC to be performed by widely used planar technology. The transition from planar to TDIC technology is explained by accumulation of knowledge of features for many strip-slot type lines [2,3,7]. The ambition to connection of this line advantages in the one construction was natural. This ambition was realized by transition to TDIC (It was taken shape in the construction correspondence principle). Second basic principle for TDIC (optimum basis element principle) was realized too [1-3].

1.2 Bilateral slot line (BSL) which has some wonderful features (fig.1a; [2,8]) is widely used in micro-wave electronics (especially in EHF range). The quasi-opened variant of BSL is of interest for TDIC (fig.1b) whose good model is a structure with virtual electrical and magnetic walls (fig.1c).

Some more generalized kinds of BSL which are of interest for TDIC are considered in this work. Firstly, symmetrical BSL with different slot widths (fig.3a) is studied. Second structure of family of BSLs is nonsymmetrical BSL (fig.3b) which is a foundation for many basis elements of TDIC.

2. Formulation of the problem. Method of partial regions.
2.1 Numerical approach. Bubnov-Galerkin's method.

The generalized double-slot waveguide (GDSW) is two slots which are cut through in infinitely thin layers of metal located on both sides of dielectric film. The structure is assumed uniform with respect to z-axis. Its cross section is shown at the fig.2a. The relative dielectric permittivity of substrate ε_r is assumed homogeneous, isotropic, constant and relative permeability $\mu_r=1$.

The structures whose geometry is shown on fig.2a is opened. The solution of Helmholtz equation with the adequate boundary conditions is the external electrodynamic problem. For simplification of formulation of the problem we will consider the GDSW in the rectangular waveguide that transform opened waveguiding structure to the structure of fin-line type. Obtaining the characteristics of opened structure is possible by removing the walls of rectangular waveguide to infinity (really, size of external rectangular waveguide must be more than λ_0).

But, establishment of "virtual" vertical electrical or (and) magnetic walls for simulation of GDSW has sense not only for simplification of problem into adjoint operator. Certainly, presence of walls simplifies formulation and solution of problem essentially. Establishment of virtual walls allows class of solutions which are not taken into account in usual analysis to be introduced for analysis. Opened lines and resonators with impedance jumps near margins of structures [11] (fig.4) are contemplated.

Creature of such jumps by "excrescences" (fig.4a) or by some impedance insertions (for example, frequently periodic or anisotropic structure [12,13] (fig.4b)) is not difficult for technology.

19980423 035

REPORT DOCUMENTATION PAGE

Form Approved OMB No. 0704-0188

1. AGENCY USE ONLY (Leave blank)	2. REPORT DATE	3. REPORT TYPE AND DATES COVERED
	1998	Final Report

4. TITLE AND SUBTITLE

Generalized Double-Slot Waveguide Components For Millimeter-Wave Integrated Circuits

5. FUNDING NUMBERS

F6170896W0266

6. AUTHOR(S)

Prof. Evgeny Nefyodov

7. PERFORMING ORGANIZATION NAME(S) AND ADDRESS(ES)

Institute of Radio Engineering and Electronics of the Russian Academy of Science
Vvedenscogo sq. 1
Fryazino 141120
Russia

8. PERFORMING ORGANIZATION REPORT NUMBER

N/A

9. SPONSORING/MONITORING AGENCY NAME(S) AND ADDRESS(ES)

EOARD
PSC 802 BOX 14
FPO 09499-0200

10. SPONSORING/MONITORING AGENCY REPORT NUMBER

SPC 96-4059

11. SUPPLEMENTARY NOTES

12a. DISTRIBUTION/AVAILABILITY STATEMENT

Approved for public release; distribution is unlimited.

12b. DISTRIBUTION CODE

A

13. ABSTRACT (Maximum 200 words)

This report results from a contract tasking Institute of Radio Engineering and Electronics of the Russian Academy of Science as follows: The contractor will investigate the Generalized double-slot waveguide components for millimeter-wave integrated circuits as described in his proposal.

DTIC QUALITY INSPECTED 4

14. SUBJECT TERMS

Computers

15. NUMBER OF PAGES

21

16. PRICE CODE

N/A

17. SECURITY CLASSIFICATION OF REPORT	18. SECURITY CLASSIFICATION OF THIS PAGE	19. SECURITY CLASSIFICATION OF ABSTRACT	20. LIMITATION OF ABSTRACT
UNCLASSIFIED	UNCLASSIFIED	UNCLASSIFIED	UL

For certain conditions, partial waves composing eigenwaves of GDSW are reflected on impedance jump (phase shift can take place through reflection process; it depend on parameters of line, λ, impedance character etc.). So, on the one hand virtual wall processes are simulated, on the other hand region of applications for this mathematic model is increased.

Now a day, many methods have presented for analysis of planar waveguiding structures [2,5,7,9]. Most widely used and multipurpose method is the method of elementary regions (ERM) which allows relations for determine the propagation constant of the structure (as the transcendental equation) to be obtained. The transcendental equation is solved by some numerical method with computer. The description of ERM is presented widely at the educational and scientific literature [2,5,8,9] in details and we will not describe this method and will detail some basic items which are most important for this problem.

Packing out the part of solution which depend on z-coordinate as $e^{-j\beta z}$ we transform our problem to two-dimensional problem. The unknown solution of the latter in the cross section of line is presented as follows:

$$\Phi^{(i)}(x,y) = \sum_n A_n^{(i)} R_n^{(i)}(x)\psi_n^{(i)}(y), \qquad (2.1.1)$$

where up index i ($i=1,2,3$) denotes number of region (see fig.2b), $R_n^{(i)}$ and $\psi_n^{(i)}$ - the eigenfunctions of Helmholtz equation in the i-th region which satisfy to boundary conditions on the walls of rectangular waveguide $\left(E_\tau\big|_S = 0, \dfrac{\partial H_n}{\partial n}\bigg|_S = 0 \right)$, $A_n^{(i)}$ - unknown coefficients.

The sets of eigenfunctions $R_n^{(i)}$ and $\psi_n^{(i)}$ have properties of plentitude and orthogonality in the corresponding regions. "Sewing together" the solutions in the neighbor regions by usual boundary conditions and using Galerkin's method we obtain the homogeneous linear algebraic equation system (LAES) with respect to unknown coefficients $\left(a_i, b_i, c_i, d_i\right)$ of decomposition by basis functions of tangential components of electrical field $\left(E_y, E_z\right)$ in the aperture of the slots:

$$\begin{bmatrix} Y_{11} & Y_{12} & Y_{13} & Y_{14} \\ Y_{21} & Y_{22} & Y_{23} & Y_{24} \\ Y_{31} & Y_{32} & Y_{33} & Y_{34} \\ Y_{41} & Y_{42} & Y_{43} & Y_{44} \end{bmatrix} \times \begin{bmatrix} a_k \\ b_k \\ c_k \\ d_k \end{bmatrix} = \vec{0} , \qquad (2.1.2)$$

where: $Y_{ij(lk)} = \sum_n G_{nij}\xi_{ln}^i\xi_{kn}^j$, $\left(i,j=\overline{1,4}\right), \left(l,k=\overline{1,N}; n=\overline{0,\infty}\right)$,

$$G_{n11} = \frac{j}{(1+\delta_{0n})}\left(\left[k_0^2\varepsilon_2 - \beta^2\right]\frac{Ctg(\gamma_{n2}d)}{\mu_2\gamma_{n2}} + \left[k_0^2\varepsilon_1 - \beta^2\right]\frac{Ctg(\gamma_{n1}h_1)}{\mu_1\gamma_{n1}} \right),$$

$$G_{n12} = -\alpha_n\beta\left(\frac{Ctg(\gamma_{n2}d)}{\mu_2\gamma_{n2}} + \frac{Ctg(\gamma_{n1}h_1)}{\mu_1\gamma_{n1}} \right),$$

$$G_{n13} = \frac{-j}{(1+\delta_{0n})}\frac{k_0^2\varepsilon_2 - \beta^2}{\mu_2\gamma_{n2}Sin(\gamma_{n2}d)},$$

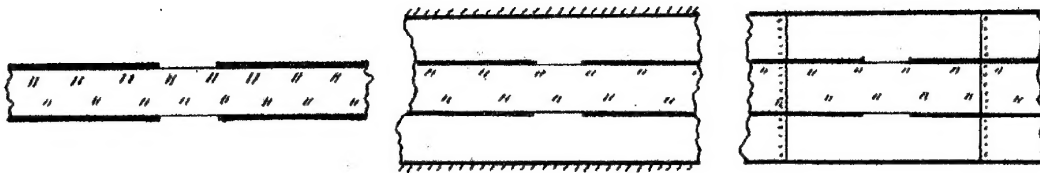a)   b)   c)

Fig. 1. Cross section of bilateral slot line (double-slot waveguide):
    a - opened structure; b - quasi-opened structure (most interest for TDIC);
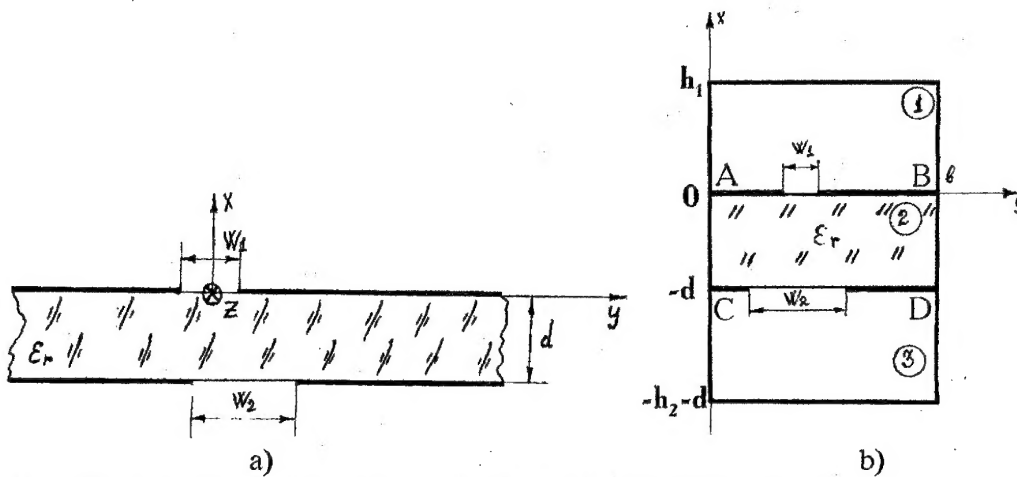   c - model of BSL.

a)   b)

Fig. 2. Cross section of generalized double-slot waveguide:
    a - opened structure; b - cross section of GDSW model.

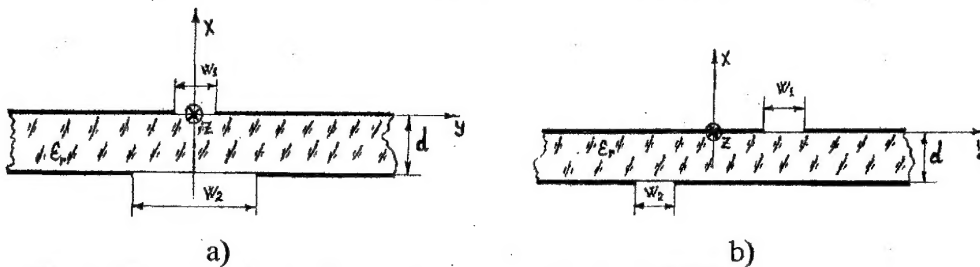a)   b)

Fig. 3. Cross sections of some important kinds of GDSW:
    a - symmetrical GDSW with the different slot widths;
    b - nonsymmetrical GDSW with the equal slot widths.

a)   b)

Fig. 4. Possible physical realizations of virtual vertical walls.
    a) By "excrescences";
    b) By impedance insertions.

$$G_{n14} = \frac{\alpha_n \beta}{\mu_2 \gamma_{n2} Sin(\gamma_{n2}d)}, \qquad G_{n21} = -G_{n12},$$

$$G_{n22} = j\left(\left[k_0^2 \varepsilon_2 - \alpha_n^2\right]\frac{Ctg(\gamma_{n2}d)}{\mu_2 \gamma_{n2}} + \left[k_0^2 \varepsilon_1 - \alpha_n^2\right]\frac{Ctg(\gamma_{n1}h_1)}{\mu_1 \gamma_{n1}}\right),$$

$$G_{n23} = -G_{n14}, \qquad G_{n24} = -j\frac{k_0^2 \varepsilon_2 - \alpha_n^2}{\mu_2 \gamma_{n2} Sin(\gamma_{n2}d)}, \; G_{n31} = G_{n13}, \; G_{n32} = -G_{n23},$$

$$G_{n33} = \frac{j}{(1+\delta_{0n})}\left(\left[k_0^2 \varepsilon_2 - \beta^2\right]\frac{Ctg(\gamma_{n2}d)}{\mu_2 \gamma_{n2}} + \left[k_0^2 \varepsilon_3 - \beta^2\right]\frac{Ctg(\gamma_{n3}h_2)}{\mu_3 \gamma_{n3}}\right),$$

$$G_{n34} = -\alpha_n \beta\left(\frac{Ctg(\gamma_{n2}d)}{\mu_2 \gamma_{n2}} + \frac{Ctg(\gamma_{n3}h_2)}{\mu_3 \gamma_{n3}}\right), G_{n41} = -G_{n14}, \; G_{n42} = G_{n24},$$

$$G_{n43} = -G_{n34}, \; G_{n44} = j\left(\left[k_0^2 \varepsilon_2 - \alpha_n^2\right]\frac{Ctg(\gamma_{n2}d)}{\mu_2 \gamma_{n2}} + \left[k_0^2 \varepsilon_3 - \alpha_n^2\right]\frac{Ctg(\gamma_{n3}h_2)}{\mu_3 \gamma_{n3}}\right),$$

$$\xi_{kn}^1 = \int_0^b E_k^{(y)}\Big|_{x=0} \cos(\alpha_n y)dy, \; \xi_{kn}^2 = \int_0^b E_k^{(z)}\Big|_{x=0} \sin(\alpha_n y)dy, \; \xi_{kn}^3 = \int_0^b E_k^{(y)}\Big|_{x=-d} \cos(\alpha_n y)dy,$$

$$\xi_{kn}^4 = \int_0^b E_k^{(z)}\Big|_{x=-d} \sin(\alpha_n y)dy, \; \alpha_n = \frac{\pi n}{b},$$

with the relation $\gamma_{ni} = \sqrt{k_0^2 \varepsilon_i \mu_i - \beta^2 - \alpha_n^2}$ taking place (i denotes the number of region).

From the condition that the solution of LAES is nontrivial we obtain dispersion equation of the structure:

$$\det\|Y\| = 0, \tag{2.1.3}$$

which must be solved with respect to free parameter β by any numerical method. The *Newton's* method was used for this purpose in our investigations.

It should be noted that, the accuracy of solution and time required for solution of (2.1.3) depend on what basis functions are chosen for description tangential electrical field in the aperture of the slots. For our investigations we have chosen *Chebyshev's* polynoms:

$$E_k^{(z)i} = \sqrt{1-\left[\frac{2}{w_i}(y-y_{ci})\right]^2} U_{2k-1}\left(\frac{2}{w_i}(y-y_{ci})\right); \quad E_k^{(y)i} = \frac{T_{2(k-1)}\left(\frac{2}{w_i}(y-y_{ci})\right)}{\sqrt{1-\left[\frac{2}{w_i}(y-y_{ci})\right]^2}}, \tag{2.1.4}$$

where i - is a number of the slot, y_{ci} - the coordinate of i-th slot center, w_i - the i-th slot width, T_k and U_k - *Chebyshev's* polynoms of first and second kinds, respectively.

2.2 Numerical-Analytical formulation. Singular Integral Equation and orthogonalization substitution methods.

Formulation of problem according to 2.1 item drive to infinite Linear Algebraic Equation System (LAES) which allows solution with any accuracy intended beforehand to be obtained after reduction procedure. But, this algorithm for great calculations (such as optimization problem of basis elements and functional units for TDIC) is successful not always. Time of calculations (even for not complex units constructively) is not satisfactory for practical synthesis needs.

Analytical-numerical approximate method for simulation of non-symmetric double-slot waveguide (NDSW) is proposed. It is based on utilization of singular integral equation (SIE), Schwinger transformation and orthogonalization substitution methods [9]. This new formulation of problem allows analytical formulation of dispersion equation for wide set of problems and sometime for propagation constants of eigenwaves of strip-slot structures to be obtained. Analytical approximation for accuracy can be written by this problem's formulation.

So, general approach for mathematic simulation of NDSW is scheduled. Namely, first step is obtaining the approximate solution. If accuracy of the solution is not satisfactory, it will be increased by any rigorous method in second step (see 2.1 item) and results of first step are used as starting values for second step.

In this report both approach according to 2.1 item and approach of 2.2 item are realized separately. Author's plans are to create synthesis algorithm for simulation of NDSW for TDIC on Microwave and EHF.

We shall assume that following conditions are valid:

$$\varepsilon^{(1)} = \varepsilon^{(3)}; \quad \mu^{(1)} = \mu^{(3)}; \quad h_1 = h_2;$$

$$y_{21} = b - y_{12}; \quad y_{22} = b - y_{11}.$$

(2.2.1)

These assumptions are correct for much constructions which are interest for practice.

If we shall make variable substitution in (2.1.2) and take into account correlation between $\ddot{\vec{G}}_n$ tensor's elements

$$G_{n44} = G_{n22}; \quad G_{n43} = G_{n21}; \quad G_{n33} = G_{n11},$$

(these correlations follow from (2.2.1) conditions), we can obtain following vector equations:

$$\sum_{n=0}^{\infty} \ddot{\vec{D}}_n(y)\widetilde{\ddot{\vec{G}}}_n \widetilde{\vec{E}}_n = 0, \quad (y_{11} < y < y_{12}),$$

(2.2.2)

where

$$\ddot{\vec{D}}_n(x) = \begin{pmatrix} Cos\left(\dfrac{n\pi}{b}y_1\right) & 0 & 0 & 0 \\ 0 & Sin\left(\dfrac{n\pi}{b}y_1\right) & 0 & 0 \\ 0 & 0 & Cos\left(\dfrac{n\pi}{b}y_2\right) & 0 \\ 0 & 0 & 0 & Sin\left(\dfrac{n\pi}{b}y_2\right) \end{pmatrix},$$

$$\widetilde{\ddot{\vec{G}}}_n = \begin{pmatrix} -G_{n11} & -G_{n12} & (-1)^{n+1}G_{n13} & (-1)^n G_{n14} \\ G_{n21} & G_{n22} & (-1)^n G_{n23} & (-1)^{n+1}G_{n24} \\ (-1)^{n+1}G_{n13} & (-1)^{n+1}G_{n14} & -G_{n11} & G_{n12} \\ (-1)^{n+1}G_{n23} & (-1)^{n+1}G_{n24} & -G_{n21} & G_{n22} \end{pmatrix},$$

$$\widetilde{\vec{E}}_n = \begin{pmatrix} \int_{y_{11}}^{y_{12}} E_y(y', x=0) \cos\dfrac{\pi n y'}{b} dy' \\[2mm] \int_{y_{11}}^{y_{12}} E_z(y', x=0) \sin\dfrac{\pi n y'}{b} dy' \\[2mm] \int_{y_{11}}^{y_{12}} E_y(b-y', x=-d) \cos\dfrac{\pi n y'}{b} dy' \\[2mm] \int_{y_{11}}^{y_{12}} E_z(b-y', x=-d) \sin\dfrac{\pi n y'}{b} dy' \end{pmatrix}.$$

All integral relations in (2.2.2) have the same range of definition which correspond to up-slot (see fig. 2b).

Eigenwave will be called odd-even if its tangential components have follow properties: $E_z(b-y,-d) = -E_z(y,0); \quad E_y(b-y,-d) = E_y(y,0)$.

Wave will be called even-odd if follow conditions are valid:
$$E_z(b-y,-d) = E_z(y,0); \quad E_y(b-y,-d) = -E_y(y,0).$$

Theorem. Odd-even and even-odd waves can propagate in NDSW.

Evidence. We will denote unknown vector function as follow:
$$\vec{e}(y) = \begin{pmatrix} E_y(y,0) \\ E_z(y,0) \\ E_y(b-y,-d) \\ E_z(b-y,-d) \end{pmatrix}.$$

Assuming that vector
$$\vec{\varphi}(y) = \begin{pmatrix} \varphi_y^{(1)}(y) \\ \varphi_z^{(1)}(y) \\ \varphi_y^{(2)}(y) \\ \varphi_z^{(2)}(y) \end{pmatrix}$$

is solution of (2.2.2); following equation is valid:
$$\sum_{n=0}^{\infty} \overset{\leftrightarrow}{\vec{D}}_n(y) \widetilde{\overset{\leftrightarrow}{G}}_n \widetilde{\vec{\Phi}}_n = 0, \quad (y_{11} < y < y_{12}), \tag{2.2.3}$$

where

$$\widetilde{\vec{\Phi}}_n = \begin{pmatrix} \int_{y_{11}}^{y_{12}} \varphi_y^{(1)}(y') \cos\dfrac{\pi n y'}{b} dy' \\[2mm] \int_{y_{11}}^{y_{12}} \varphi_z^{(1)}(y') \sin\dfrac{\pi n y'}{b} dy' \\[2mm] \int_{y_{11}}^{y_{12}} \varphi_y^{(2)}(y') \cos\dfrac{\pi n y'}{b} dy' \\[2mm] \int_{y_{11}}^{y_{12}} \varphi_z^{(2)}(y') \sin\dfrac{\pi n y'}{b} dy' \end{pmatrix} .$$

It is not difficult to obtain, the substitution of

$$\vec{\varphi}'(y) = \begin{pmatrix} -\varphi_y^{(2)}(y) \\[2mm] \varphi_z^{(2)}(y) \\[2mm] -\varphi_y^{(1)}(y) \\[2mm] \varphi_z^{(1)}(y) \end{pmatrix}$$

in (2.2.2) drive to (2.2.3) too. So, $\vec{\varphi}(y)$ and $\vec{\varphi}'(y)$ satisfy the system (2.2.2) simultaneously. But linearity of integral relations (2.2.2) allows to talk the same about $\vec{\varphi}(y) - \vec{\varphi}'(y)$ and $\vec{\varphi}(y) + \vec{\varphi}'(y)$ (the former correspond to odd-even mode, the latter correspond to even-odd mode). *The evidence is finished.*

From this theorem we can see, integral relations (2.2.2) are resolved into two independent systems:

$$\sum_{n=0}^{\infty} \vec{\vec{L}}_n(y) \vec{\vec{R}}_n \vec{p}_n = 0, \quad (y_{11} < y < y_{12}), \tag{2.2.4}$$

where

$$\vec{\vec{L}}_n = \begin{pmatrix} \sin\dfrac{\pi n y}{b} & 0 \\[3mm] 0 & \cos\dfrac{\pi n y}{b} \end{pmatrix} ; \quad \vec{p}_n = \begin{pmatrix} \int_{y_{11}}^{y_{12}} E_z(y',0) \sin\dfrac{\pi n y'}{b} dy' \\[3mm] \int_{y_{11}}^{y_{12}} E_y(y',0) \cos\dfrac{\pi n y'}{b} dy' \end{pmatrix} ;$$

$$\vec{\vec{R}}_n = \begin{pmatrix} G_{n22} \pm (-1)^n G_{n24} & G_{n21} \pm (-1)^n G_{n23} \\[2mm] G_{n12} \pm (-1)^n G_{n14} & G_{n11} \pm (-1)^n G_{n13} \end{pmatrix} .$$

Up-index in definition of $\vec{\vec{R}}_n$ tensor correspond to odd-even mode and sub-index correspond to even-odd modes.

So, eigenwave problem for NDSW is transformed to boundary problem for waveguide-slot transmission line where $\vec{\vec{R}}_n$ has been chosen as metal surface admittance tensor in [9].

Converting the integral operator. Integration by parts converts problem from (2.2.4) form into first kind integral equation system as follow:

$$\int_{y_{11}}^{y_{12}}\left[\sum_{n=1}^{\infty}\frac{b}{\pi n}R_{n11}\cos\frac{\pi ny'}{b}\sin\frac{\pi ny}{b}E_z'(y')+\sum_{n=1}^{\infty}R_{n12}\cos\frac{\pi ny'}{b}\sin\frac{\pi ny}{b}E_y(y')\right]dy'=0$$

$$\int_{y_{11}}^{y_{12}}\left[\sum_{n=1}^{\infty}\frac{b}{\pi n}R_{n21}\cos\frac{\pi ny'}{b}\cos\frac{\pi ny}{b}E_z'(y')+\sum_{n=0}^{\infty}R_{n22}\cos\frac{\pi ny'}{b}\cos\frac{\pi ny}{b}E_y(y')\right]dy'=0$$

$$(y_{11}<y<y_{12})\qquad\qquad(2.2.5)$$

where following indexes are introduced: $E_z'(y)=\dfrac{d}{dy}E_z(y,0);\quad E_y(y)=E_y(y,0).$

Taking into account asymptotic behavior of $\ddot{R}_n$ tensor for $n\to\infty$:

$$R_{n11}\sim nt_1;\quad R_{n12}=R_{n21}\sim t_2;\quad R_{n22}\sim t_3\big/n,$$

where

$$t_1=\frac{2\pi i}{kb^2}\left(\frac{1}{\mu^{(1)}}+\frac{1}{\mu^{(2)}}\right);\quad t_2=-\frac{2\beta}{kb}\left(\frac{1}{\mu^{(1)}}+\frac{1}{\mu^{(2)}}\right);$$

$$t_3=\frac{2i}{\pi k}\left[\frac{\left(\alpha_0^{(1)}\right)^2}{\mu^{(1)}}+\frac{\left(\alpha_0^{(2)}\right)^2}{\mu^{(2)}}\right],$$

we can isolate singularities in cores of integral equations (2.2.5):

$$\int_{y_{11}}^{y_{12}}\left\{\sum_{n=1}^{\infty}\frac{b}{\pi}\left(\frac{1}{n}R_{n11}-t_1\right)\cos\frac{\pi ny'}{b}\sin\frac{\pi ny}{b}E_z'(y')+\right.$$

$$\left.+\sum_{n=1}^{\infty}\left(R_{n12}-t_2\right)\cos\frac{\pi ny'}{b}\sin\frac{\pi ny}{b}E_y(y')\right\}dy'=$$

$$=-\frac{1}{2}\int_{y_{11}}^{y_{12}}\frac{\sin\dfrac{\pi y}{b}}{\cos\dfrac{\pi y'}{b}-\cos\dfrac{\pi y}{b}}\left[\frac{b}{\pi}t_1E_z'(y')+t_2E_y(y')\right]dy';$$

$$\int_{y_{11}}^{y_{12}}\left\{\sum_{n=1}^{\infty}\frac{b}{\pi n}\left(R_{n21}-t_2\right)\cos\frac{\pi ny'}{b}\cos\frac{\pi ny}{b}E_z'(y')+\left[R_{022}+\right.\right.\qquad(2.2.6)$$

$$\left.\left.+\sum_{n=1}^{\infty}\left(R_{n22}-\frac{t_3}{n}\right)\cos\frac{\pi ny'}{b}\cos\frac{\pi ny}{b}\right]E_y(y')\right\}dy'=$$

$$=\frac{1}{2}\int_{y_{11}}^{y_{12}}\ln\left|2\left(\cos\frac{\pi y'}{b}-\cos\frac{\pi y}{b}\right)\right|\cdot\left[\frac{b}{\pi}t_2E_z'(y')+t_3E_y(y')\right]dy',$$

$$(y_{11}<y<y_{12}).$$

Following relations were used here:

$$\sum_{n=1}^{\infty} cos\frac{\pi n y'}{b} sin\frac{\pi n y}{b} = \frac{1}{2} \frac{sin\dfrac{\pi y}{b}}{cos\dfrac{\pi y'}{b} - cos\dfrac{\pi y}{b}};$$

$$\sum_{n=1}^{\infty} \frac{1}{n} cos\frac{\pi n y'}{b} cos\frac{\pi n y}{b} = -\frac{1}{2} ln\left|2\left(cos\frac{\pi y'}{b} - cos\frac{\pi y}{b}\right)\right|.$$

Infinite sums in left parts of (2.2.6) converge to limited functions in $\left[y_{11} < y < y_{12}\right] \times \left[y_{11} < y' < y_{12}\right]$ square, it is essential.

With an eye to these series can be orthogonal decomposition on range of definition, we use orthogonal substitution for (2.2.6) as follow [9]:

$$cos\frac{\pi y}{b} = c + su; \quad cos\frac{\pi y'}{b} = c + sv,$$

where

$$c = \frac{1}{2}\left(cos\frac{\pi y_{11}}{b} + cos\frac{\pi y_{12}}{b}\right); \quad s = \frac{1}{2}\left(cos\frac{\pi y_{11}}{b} - cos\frac{\pi y_{12}}{b}\right).$$

We shall obtain:

$$\frac{1}{\pi}\int_{-1}^{1}\frac{1}{v-u}\left[t_1 e_z'(v) + t_2 e_y(v)\right]dv = -\frac{2s}{\pi}\int_{-1}^{1}\left\{\sum_{n=1}^{\infty}\left(\frac{1}{n}R_{n11} - t_1\right)\cdot\right.$$

$$\cdot T_n(c+sv)U_{n-1}(c+su)e_z'(v) + \sum_{n=1}^{\infty}\left(R_{n12} - t_2\right)T_n(c+sv)\cdot$$

$$\cdot U_{n-1}(c+su)e_y(v)\Big\}dv;$$

$$\frac{1}{\pi}\int_{-1}^{1}ln|v-u|\cdot\left[t_2 e_z'(v) + t_3 e_y(v)\right]dv = \frac{1}{\pi}\int_{-1}^{1}\left\{\left[-t_2 ln2s + 2\sum_{n=1}^{\infty}\frac{1}{n}\cdot\right.\right. \quad (2.2.7)$$

$$\cdot\left(R_{n21} - t_2\right)T_n(c+sv)T_n(c+su)\Big]e_z'(v) + \Big[2R_{022} - t_3 ln2s +$$

$$+ 2\sum_{n=1}^{\infty}\left(R_{n22} - \frac{t_3}{n}\right)T_n(c+sv)T_n(c+su)\Big]e_y(v)dv, \quad (-1 < u < 1),$$

where

$$e_z'(v) = \frac{1}{\sqrt{1-(c+sv)^2}}\frac{b}{\pi}E_z'\left(\frac{b}{\pi}arccos(c+sv)\right);$$

$$e_y(v) = \frac{1}{\sqrt{1-(c+sv)^2}}E_y\left(\frac{b}{\pi}arccos(c+sv)\right),$$

T_n, U_n - Chebyshev's polynoms of first and second kinds, respectively.

Solutions of integral equations:

$$\frac{1}{\pi}\int_{-1}^{1}\frac{\varphi(v)}{v-u}dv = f(u), \quad (-1 < u < 1);$$

$$\frac{1}{\pi}\int_{-1}^{1} ln|v-u|\psi(v)dv = g(u), \quad (-1 < u < 1)$$

can be presented as [9]:

$$\varphi(u) = \frac{a_0}{\sqrt{1-u^2}} - \frac{1}{\pi\sqrt{1-u^2}}\int_{-1}^{1}\frac{\sqrt{1-v^2}}{v-u}f(v)dv;$$

$$\psi(u) = \frac{1}{\pi\sqrt{1-u^2}}\left[\int_{-1}^{1}\frac{\sqrt{1-v^2}}{v-u}g'(v)dv - \frac{1}{ln2}\int_{-1}^{1}\frac{g(v)}{\sqrt{1-v^2}}dv\right],$$

where a_0 - is arbitrary constant.

Using these relations, we can convert integral operator in (2.2.7). Result is a system of integral equations of second kind:

$$t_1 e_z'(u) + t_2 e_y(u) = \frac{a_0}{\sqrt{1-u^2}} + \frac{2s}{\pi^2\sqrt{1-u^2}}\int_{-1}^{1}\left\{\sum_{n=1}^{\infty}\left(\frac{1}{n}R_{n11} - t_1\right)\cdot\right.$$

$$\left.\cdot T_n(c+sv)\Omega_n(u)e_z'(v) + \sum_{n=1}^{\infty}(R_{n12} - t_2)T_n(c+sv)\Omega_n(u)e_y(v)\right\}dv; \quad (2.2.8)$$

$$t_2 e_z'(u) + t_3 e_y(u) = \frac{1}{\pi^2\sqrt{1-u^2}}\int_{-1}^{1}\left\{\left[\pi t_2\frac{ln2s}{ln2} + 2\sum_{n=1}^{\infty}\frac{1}{n}(R_{n21} - t_2)\cdot\right.\right.$$

$$\left.\cdot\left(sn\Omega_n(u) - \frac{1}{ln2}\Lambda_n\right)T_n(c+sv)\right]e_z'(v) + \left[-\frac{\pi}{ln2}(2R_{022} - t_3 ln2s) + \right.$$

$$\left.\left. + 2\sum_{n=1}^{\infty}\left(R_{n22} - \frac{t_3}{n}\right)\left(sn\Omega_n(u) - \frac{1}{ln2}\Lambda_n\right)T_n(c+sv)\right]e_y(v)\right\}dv, \quad (2.2.9)$$

$$(-1 < u < 1)$$

where

$$\Omega_n(u) = \int_{-1}^{1}\frac{\sqrt{1-v^2}}{v-u}U_{n-1}(c+sv)dv;$$

$$\Lambda_n = \int_{-1}^{1}T_n(c+sv)\frac{dv}{\sqrt{1-v^2}}.$$

Dispersion equation. Truncation of series in cores (taking into account first N terms only) drive (2.2.8), (2.2.9) into degenerate integral equation system. Algebraization of this system with utilization of Chebyshev's polynoms as basis functions:

$$e_z'(u) = \frac{1}{\sqrt{1-u^2}}\sum_{n=1}^{N}e_{zn}'T_n(u); \quad (2.2.10)$$

$$e_y(u) = \frac{1}{\sqrt{1-u^2}}\sum_{n=0}^{N}e_{yn}T_n(u), \quad (2.2.11)$$

allows nearly accurate solution to be obtained.

It is necessary to note that under substitution of (2.2.10) and (2.2.11) equation (2.2.8) will produce N algebraic equations and (2.2.9) will provide *(N+1)* equations be-

cause of presence of free parameter a_0. Absence of term with $T_0(u)$ in (2.2.10) follows from near edge condition.

For first approximation *(N=1)*, described algorithm lead to following dispersion equation for eigenwave propagation constant:

$$\begin{vmatrix} -\left[t_1 + s^2\left(R_{111} - t_1\right)\right] & -2cs\left(R_{112} - t_2\right) & -\left[t_2 + s^2\left(R_{112} - t_2\right)\right] \\ cs\left(R_{121} - t_2\right) & 2c^2\left(R_{122} - t_3\right) + 2R_{022} - t_3\,ln\,s & cs\left(R_{122} - t_3\right) \\ -\left[t_2 + s^2\left(R_{121} - t_2\right)\right] & -2cs\left(R_{122} - t_3\right) & -\left[t_3 + s^2\left(R_{122} - t_3\right)\right] \end{vmatrix} = 0.$$

$$(2.2.12)$$

Utilization of method of almost full operator's conversion for analysis of NDSW allows more simple electrodynamic theory of NDSW to be built. Dispersion equation obtained can be used as a foundation for synthesis of devices with NDSW as a foundation.

Proposed formulation of problem can be used for creature of closed guiding structure with two conductive strips located in different planes theory without some essential changes.

2.3. Determination of characteristic impedance is based on equation widely known

from circuit theory:
$$Z = \frac{U^2}{2P},$$
$$(2.3.1)$$

where U - maximum voltage in cross section of TL; P - real part of z-component of complex power.

We have from definition of voltage following:
$$U = \int\limits_{L_{ap.}} E_y dy = \widetilde{E}_y\Big|_{\alpha=0},$$
$$(2.3.2)$$

where $\widetilde{E}_y$ - is Fourier's transform of y-component of aperture field.

Complex power is determined as follow:
$$\widetilde{P} = \frac{1}{2} \int\limits_{-d-h_2}^{h_1} \int\limits_{0}^{b} \left[E_x H_y^* - E_y H_x^*\right] dy dx,$$
$$(2.3.3)$$

where up-index * denotes complex conjugation.

Complex power is written after some transformations as follow:
$$P = P_1 + P_2 + P_3,$$
$$(2.3.4)$$

where:

$$P_1 = \frac{1}{b\omega\mu_0}\sum_{n=0}^{\infty}\left[\left(\beta\left(k_0^2\varepsilon_1\mu_1 - \beta^2\right)\left(\xi_n^1\right)^2 - \beta\left(k_0^2\varepsilon_1\mu_1 - \alpha_n^2\right)\left(\xi_n^2\right)^2 + 2j\alpha_n^2\beta^2\xi_n^1\xi_n^2\right)\frac{h_1}{\gamma_{n1}^2 Sin^2\left(\gamma_{n1}h_1\right)} - \right.$$

$$\left. -\left(\beta\left(\gamma_{n1}^2 - \alpha_n^2\right)\left(\xi_n^1\right)^2 + \beta\left(k_0^2\varepsilon_1\mu_1 - \alpha_n^2\right)\left(\xi_n^2\right)^2 - 2j\alpha_n\left(k_0^2\varepsilon_1\mu_1 - \alpha_n^2\right)\xi_n^1\xi_n^2\right)\frac{Ctg\left(\gamma_{n1}h_1\right)}{\gamma_{n1}^3}\right],$$

$$P_2 = \frac{1}{b\omega\mu_0}\sum_{n=0}^{\infty}\left[\left\{\beta\left(\left(k_0^2\varepsilon_2\mu_2 - \beta^2\right)\left(\left(\xi_n^1\right)^2 + \left(\xi_n^3\right)^2\right) - \left(k_0^2\varepsilon_2\mu_2 - \alpha_n^2\right)\left(\left(\xi_n^2\right)^2 + \left(\xi_n^4\right)^2\right)\right) + \right.\right.$$

$$\left. +2j\alpha_n\beta^2\left(\xi_n^1\xi_n^2 + \xi_n^3\xi_n^4\right)\right\}\frac{d}{\gamma_{n2}^2 Sin^2\left(\gamma_{n2}d\right)} + 2\beta\left\{\left(\left(k_0^2\varepsilon_2\mu_2 - \alpha_n^2\right)\xi_n^2\xi_n^4 - \left(k_0^2\varepsilon_2\mu_2 - \beta^2\right)\xi_n^1\xi_n^3\right) - \right.$$

$$-2j\alpha_n\beta^2\left(\xi_n^3\xi_n^2+\xi_n^1\xi_n^4\right)\Big\}\frac{dCtg(\gamma_{n2}d)}{\gamma_{n2}^2Sin(\gamma_{n2}d)}+\left\{-\beta\left(\left(k_0^2\varepsilon_2\mu_2-\alpha_n^2\right)\left(\left(\xi_n^2\right)^2+\left(\xi_n^4\right)^2\right)+\right.\right.$$

$$+\left(\gamma_{n2}^2-\alpha_n^2\right)\left(\left(\xi_n^1\right)^2\dot{+}\left(\xi_n^3\right)^2\right)\bigg)+2j\alpha_n\left(k_0^2\varepsilon_2\mu_2-\alpha_n^2\right)\xi_n^1\xi_n^2+\xi_n^3\xi_n^4\bigg)\bigg\}\frac{Ctg(\gamma_{n2}d)}{\gamma_{n2}^3}+$$

$$+2\Big\{\beta\Big(\left(\gamma_{n2}^2-\alpha_n^2\right)\xi_n^1\xi_n^3+\left(k_0^2\varepsilon_2\mu_2-\alpha_n^2\right)\xi_n^2\xi_n^4\Big)-j\alpha_n\left(k_0^2\varepsilon_2\mu_2-\alpha_n^2\right)\left(\xi_n^3\xi_n^2+\xi_n^1\xi_n^4\right)\Big\}\frac{1}{\gamma_{n2}^3Sin(\gamma_{n2}d)}\Bigg],$$

$$P_3=\frac{1}{b\omega\mu_0}\sum_{n=0}^{\infty}\Bigg[\left(\beta\left(k_0^2\varepsilon_3\mu_3-\beta^2\right)\left(\xi_n^3\right)^2-\beta\left(k_0^2\varepsilon_3\mu_3-\alpha_n^2\right)\left(\xi_n^4\right)^2+2j\alpha_n^2\beta^2\xi_n^3\xi_n^4\right)\frac{h_2}{\gamma_{n3}^2Sin^2(\gamma_{n3}h_2)}-$$

$$-\left(\beta\left(\gamma_{n3}^2-\alpha_n^2\right)\left(\xi_n^3\right)^2+\beta\left(k_0^2\varepsilon_3\mu_3-\alpha_n^2\right)\left(\xi_n^4\right)^2-2j\alpha_n\left(k_0^2\varepsilon_3\mu_3-\alpha_n^2\right)\xi_n^3\xi_n^4\right)\frac{Ctg(\gamma_{n3}h_2)}{\gamma_{n3}^3}\Bigg],$$

$$\xi_n^j=\sum_{i=0}^{N}\xi_{in}^j\ \ (\text{see }(2.1.2)).$$

3. Some results.

3.1. Some test examples.

For testing the results obtained by work program the set of widely known results for different electrodynamic waveguiding structures was calculated. Electrodynamic characteristics as test examples were calculated for structures presented in [2,8].

Classic fin-line was researched as a first example. Fig. 5 shows characteristics of this line. Curves presented on fig.5ab coincide with corresponding dependences from fig.4.1 in [8] (fig.5c) for normalized wavelength and characteristic impedance.

Dependences characterizing wavelength in double-slot waveguide are shown on fig.6a (analog fig.5.1 from [8] is presented on fig.6b). Characteristics of bilateral slot line with arbitrary located slot are presented on fig.7a, their analog from [8] is on fig.7b. Conjunction of results is obvious.

Third example is antipodal (nonsymmetric) slot line whose parameters are equal to one from fig.1.20 in [2]. Results of our calculations are on fig.8a and control results are on fig.8b.

a)

b)

c)
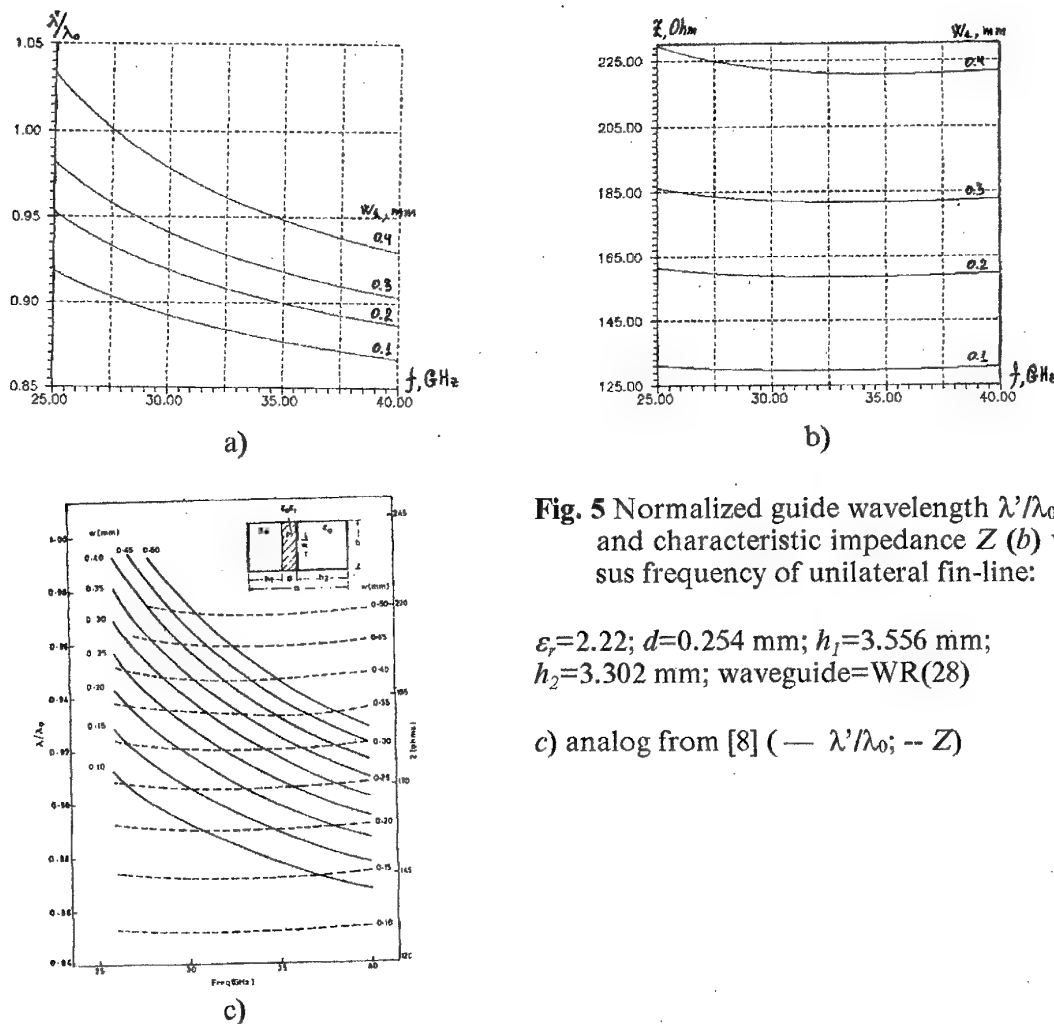
Fig. 5 Normalized guide wavelength λ'/λ_0 (a) and characteristic impedance Z (b) versus frequency of unilateral fin-line:

ε_r=2.22; d=0.254 mm; h_1=3.556 mm; h_2=3.302 mm; waveguide=WR(28)
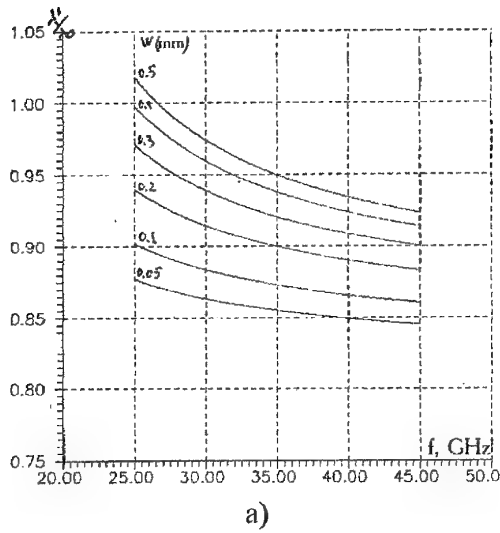
c) analog from [8] (— λ'/λ_0; -- Z)

a)

b)

Fig. 6 Normalized guide wavelength λ'/λ_0 (*a*) versus frequency of bilateral fin-line and analog from [8] (*b*):

ε_r=2.22; *d*=0.254 mm (see fig.2b); h_1=h_2=3.429 mm; waveguide=WR(28) (for fig.6b — λ'/λ_0)
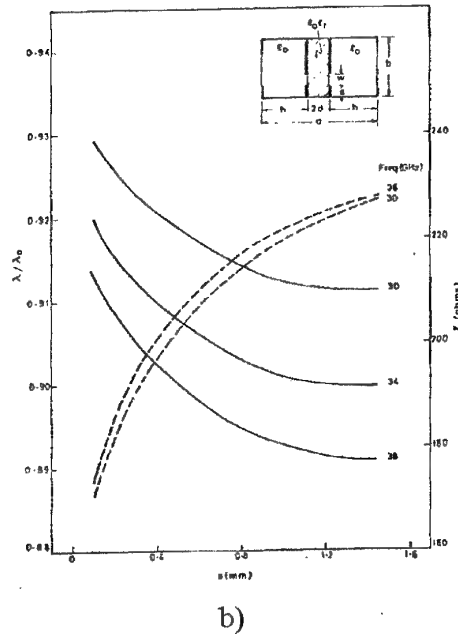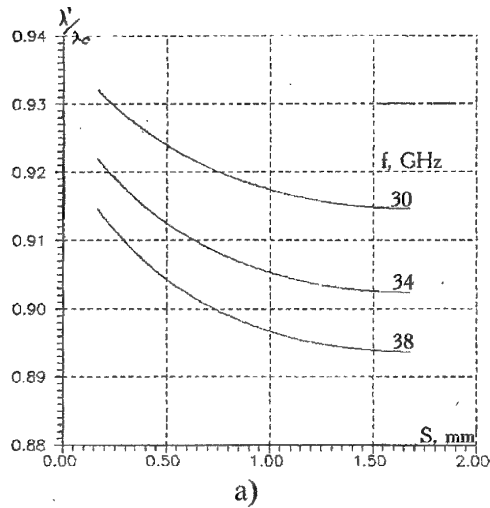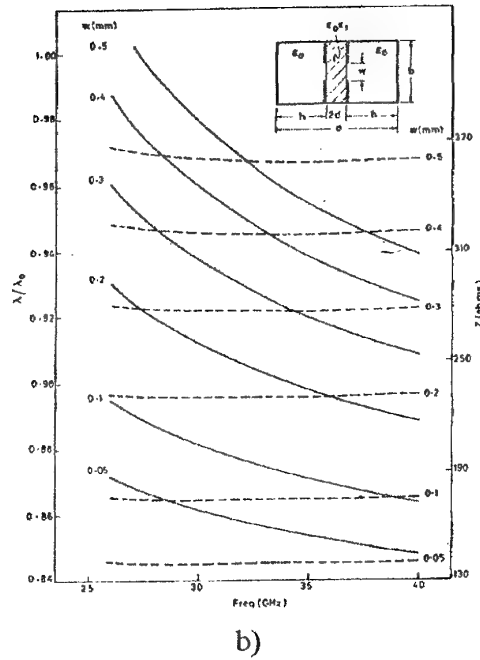

a)

b)

Fig. 7 Effect of displacing the slot on the normalized guide wavelength λ'/λ_0:
ε_r=2.22; *d*=0.254 mm (see fig.2b); h_1=h_2=3.429 mm; w_1=w_2=0.2 mm; waveguide=WR(28)

a)

b)
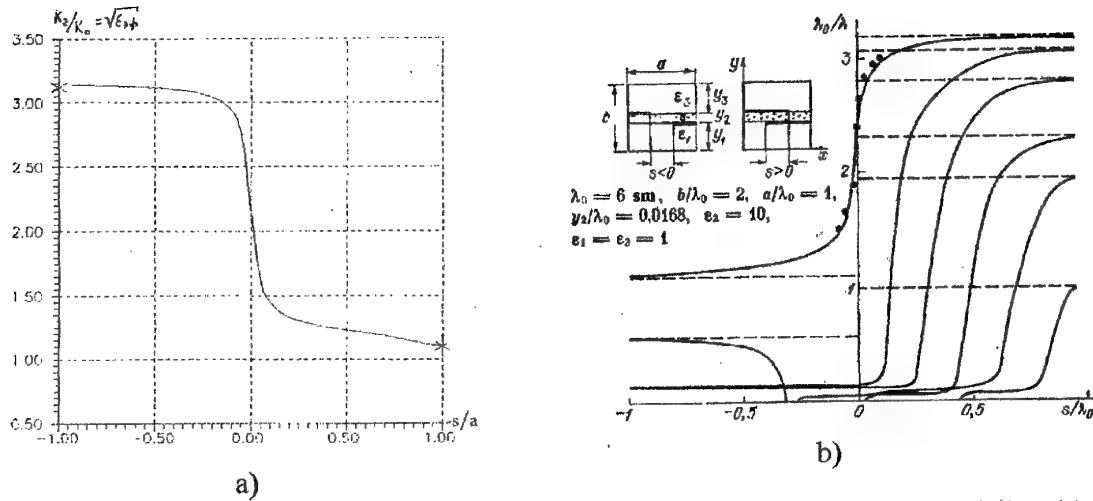
Fig. 8 Effective permittivity for slowest mode of antipodal (nonsymmetric) line (*a*) and analog from [2] (*b*); Geometrical parameters are on *b*.
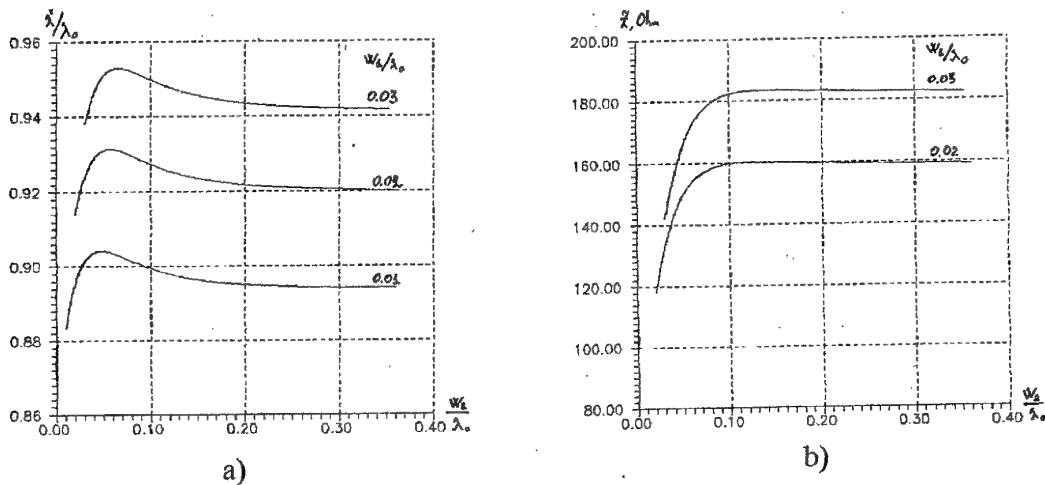

a)

b)

Fig. 9 Normalized wavelength (*a*) and characteristic impedance (*b*) of symmetric GDSW with different slot widths versus normalized w_2:

ε_r=2.22; *d*=0.254 mm (see fig.2b); h_1=h_2=3.429 mm; waveguide=WR(28)
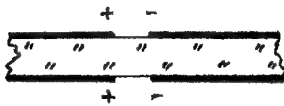

Fig. 10 Excitation of even mode of bilateral slot line.

3.2. Symmetric double-slot waveguide with different slot widths.

Fig.9a shows normalized wavelength in symmetrical GDSW with different slot widths versus normalized width of second slot w_2 (width of first slot w_1 is constant). Corresponding geometrical parameters are presented under figure. Extreme right points of curves correspond to w_2=b, that is classic fin-line. These test points agree very good with corresponding results in [8]. Extreme left points of curves are bilateral slot line exited as shown on fig.10 (even mode). These results agree with corresponding in [8] too.

Tangential components of aperture electric field for point corresponding to fin-line are presented on fig.11a. It should be noted that scaling factors for different components are different on presented figure, consequently it is not possible to discourse about ratios between components. Following consistent pattern presents for components of aperture fields: $E_{y1} \succ E_{y2}$; $E_{y2} \succ\succ E_{z2}$; $E_{z2} \succ\succ E_{z1}$. It can be noted, E field is concentrated around aperture of first (more narrow) slot predominatingly. It corresponds to classic fin-line. Longitudinal components are not drawn because of their amplitudes are negligible with compare to E_y.

As second slot w_2 become more narrow, tangential components of aperture field change according to fig.11b. Aperture distribution is not changed qualitatively, but slight increasing the E_{y2} with compare to E_{y1} is observed.

After w_2 pass acclivous region of dependence (about before $w_2/w_1 \sim 6\div 8$), phase velocity of guided wave increases. Behaviour of E_{y2} changes qualitatively (fig.11c). Before, singularity of E_{y2} near edges of second slot was absent (because of negligible amplitude of electric field in this region is). The more narrow w_2 becomes the more essential this singularity is (fig.11d). When geometry of structure reaches $w_2 = w_1$ condition following conditions take place: $E_{y1} = E_{y2}$; $E_{z1} = E_{z2}$; $E_{yi} \succ\succ E_{zi}$. Corresponding aperture field distribution is presented on fig.11e.

Current density distribution on metal is interest. Current density distribution for classic fin-line ($w_2 = b$) is shown on fig.12a. Analogously as for aperture field, scaling factors for different components are different. Following relations among components are present: $I_{z1} \succ I_{z2} \succ\succ I_{y1} \succ I_{y2}$.

Fig.12b shows current density distributions which correspond to aperture field distribution presented on fig.11b. Analogously as for field distribution, current distribution is not changed qualitatively on smooth sector of curve. I_{z2} increases slightly with respect to I_{z1}. Furthermore, current distribution is not changed as long as curve of normalized wavelength reaches its maximum (fig.12c).

Behaviour of I_{y2} begins to change hardly as maximum of curve on fig.9a will be reached (fig.12d). Further, current distribution becomes like to distribution of even mode of bilateral slot line (fig.12e).

All data presented here was shown by line with geometrical parameter of external waveguide $b = 3.5\lambda_0$. It is not actual for real devices on TDIC.

Question of side wall influence on GDSW characteristics was explored by authors fairly in details. It was obtained that behaviour of wavelength characteristics and characteristic impedance are not changed qualitatively as long as propagation of H_{10}-mode in structure formed by dielectric (ε_r) and metal on boundaries of regions 1-2 and 2-3 (rectangular\waveguide ABCD on fig.2b) is possible. See fig.13 (where $b = 0.5\lambda_0$) for comparison with fig.9, also see fig.14a (where family of curves is built with b as vary parameter).

ABCD structure (fig.2b) forms rectangular waveguide which is filled by dielectric with permittivity ε_r. Two slots are cut in wide walls of this waveguide symmetrically with respect to center of structure. As second slot becomes more narrow, the velocity of wave stipulated by ABCD becomes slower, but narrow slot enacts main role in guiding the wave yet (main guided power is concentrated near this slot). When second slot width reaches some value, guided energy is not concentrated around slots already and is directed by H_{10}-mode in rectangular waveguide. Fig.14b shows behaviour of first three roots of dispersion equation (2.1.3). It is seen that root determined by slot guided wave is third only when both slots are fairly narrow. Slowest mode is H_{10}-mode of waveguide mentioned before.
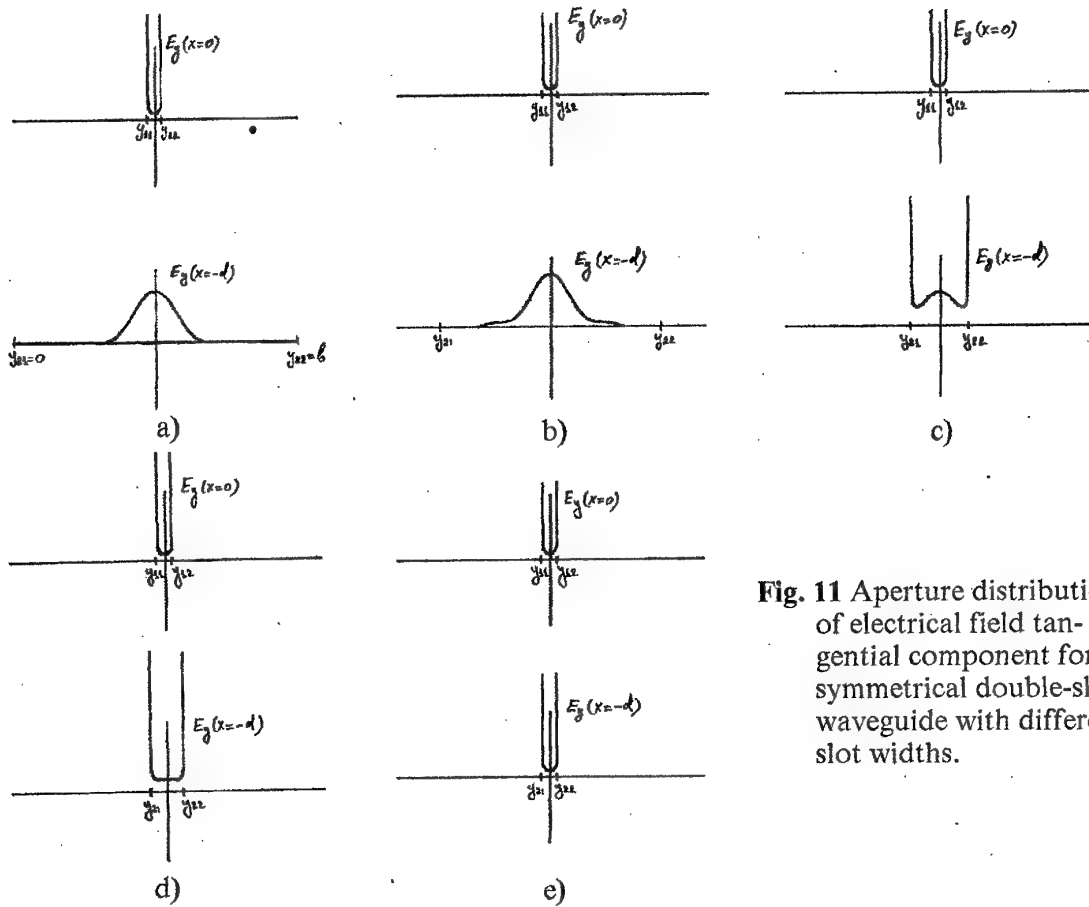
Fig. 11 Aperture distribution of electrical field tangential component for symmetrical double-slot waveguide with different slot widths.

3.3. Nonsymmetric double-slot waveguide (NDSW).

Fig.15a,b shows normalized wavelength and characteristic impedance of NDSW versus normalized distance between centers of slots $s/\lambda_0 = \dfrac{y_{11} + y_{12} - y_{21} - y_{22}}{2\lambda_0}$. In this case, $w_1 = w_2$ is assumed that satisfy to practical needs adequately. Corresponding ε_r for each curve are presented ibidem.

Extreme left point of curve corresponds to even mode of bilateral slot line (see fig.10). Results agree with corresponding one from [8].

Aperture distributions of tangential components and current densities was built through research of NDSW (like to structure described in 3.2 item). Distribution of $E_x\left(y, x = -\dfrac{d}{2}\right)$ was built additionally. Resolution of all mentioned before data was conduced authors to deduction that right sector of curve on fig.15a corresponds to wave like one guided by strip-line (with strip width equal to overlap value and substrate thickness $d/2$ (fig.2b)). Furthermore, if metal overlaps (for example $y_{11} > y_{22}$), wavelength depends on slot width $w = w_1 = w_2$ slightly for narrow slot and nearly no depends for more wide slot (see fig.16, where dashed line is characteristic of strip line). Increasing the discrepancy of NDSW characteristics and strip characteristic in extreme right point is because of closing the wall.

As b is increased, qualitative behaviour of characteristics is not changed. Wavelength of slowest wave (for $s/\lambda_0 > 0.1$, see fig.16) can be described by simple relation:

$$2\varepsilon_{eff} = \varepsilon_r + 1 + \frac{\varepsilon_r - 1}{\sqrt{1 + 10\dfrac{d}{2s}}}, \qquad (3.3.1)$$

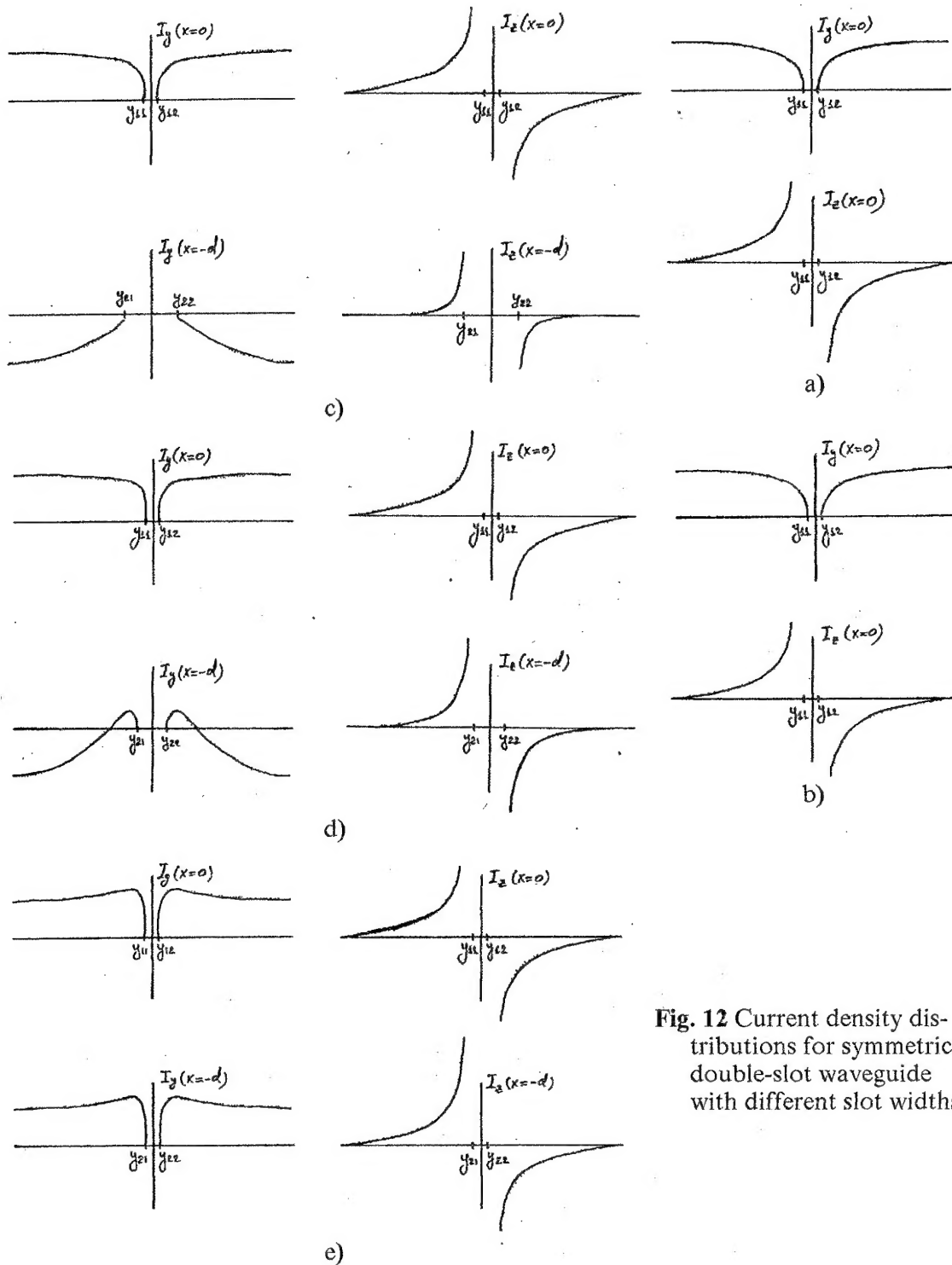where $s = y_{11} - y_{22}$. It is this formula that is shown on fig.16 by dashed line [2].

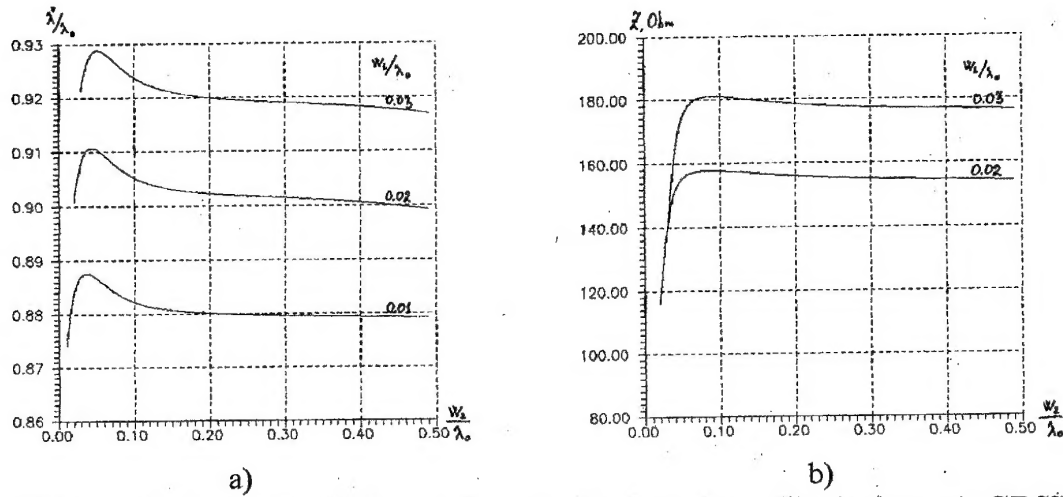**Fig. 12** Current density distributions for symmetrical double-slot waveguide with different slot widths.

a)   b)

Fig. 13 Normalized wavelength (*a*) and characteristic impedance (*b*) of symmetric GDSW
with different slot widths versus normalized w_2:
ε_r=2.22; *d*=0.254 mm; h_1=h_2=3.429 mm; *b*=0.5 λ_0

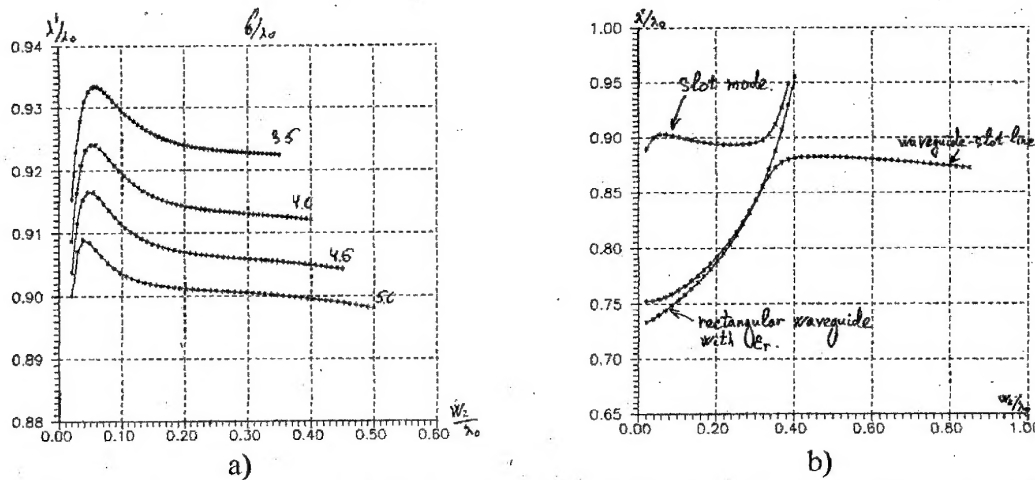
a)   b)

Fig. 14 Normalized wavelength (*a*) of symmetric GDSW with different slot widths versus
normalized w_2: ε_r=2.22; *d*=0.254 mm; h_1=h_2=3.429 mm; w_1=0.02 λ_0
b) Behaviour of first three roots of dispersion equation: ε_r=2.22; *d*=0.254 mm;
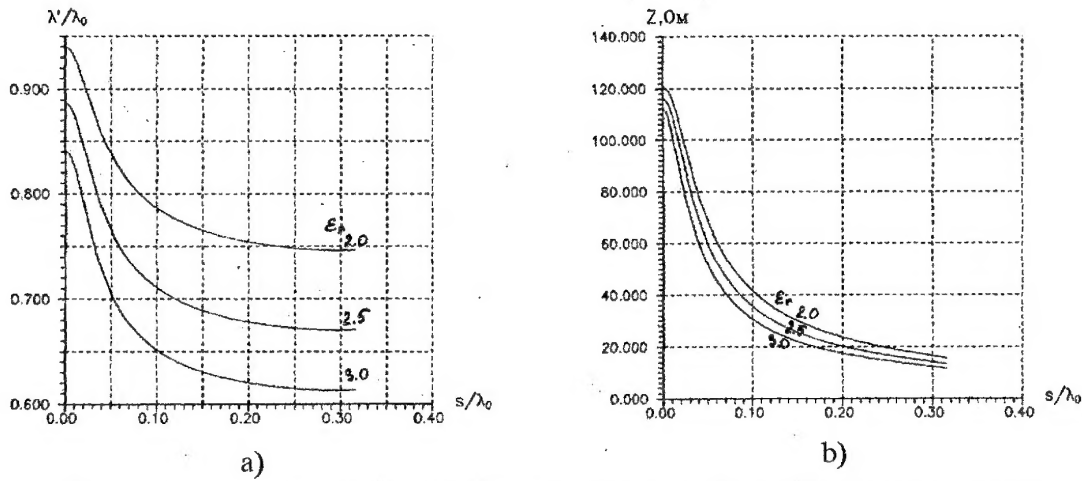h_1=h_2=3.429 mm; w_1=0.01λ_0

Fig. 15 Normalized wavelength (*a*) and characteristic impedance (*b*) of nonsymmetric GDSW versus normalized *s*:

$$\frac{s}{\lambda_0} = \frac{y_{11} + y_{12} - y_{21} - y_{22}}{2\lambda_0},$$

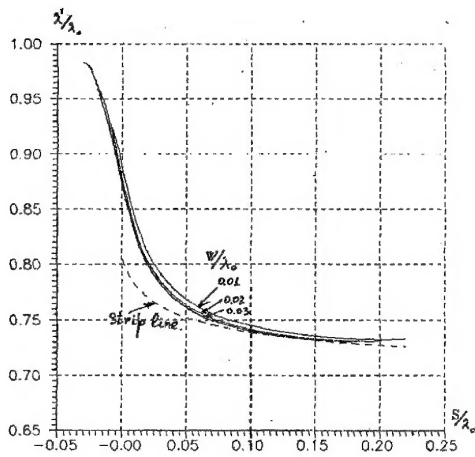*d*=0.254 mm; *h₁*=*h₂*=3.429 mm; *b*=0.35 λ₀

Fig. 16 Normalized wavelength of nonsymmetric double-slot waveguide versus overlap of metal:

ε_r=2.22; *d*=0.254 mm; *h₁*=*h₂*=3.429 mm; *s*=*y₁₁*-*y₂₂*

4. Conclusion.

The investigated variants of GDSW are the primary interest for utilization in the TDIC technology on microwave and EHF. For example, results obtained in 3.2 item (namely, research of dispersion equation roots) can be useful in questions of technology allowances etc. and method developed and described in 2.2 item is very potent and useful in the area of CAD systems for TDIC on Microwave and EHF design.

The authors are very grateful Dr.Ph. M.Davidovitz for attention for our work.

5. References

1. *Nefyodov E.I.* Radioelectronics today. - Moscow: Science, 1986. (Rus.)
2. *Gvozdev V.I., Nefyodov E.I.* Three - Dimensional integrated circuits on microwave. - Moscow: Science, 1985. (Rus.)
3. *Nefyodov E.I.* Electrodynamics of three-dimensional integrated circuits on microwave and EHF. //Radio Eng. & Electronics, 1993, vol. 38, №4, pp. 593-635. (Rus)
4. *Hirano M., Nishikawa K., etc.* Three-Dimensional passive circuit technology for ultra-compact MMIC's // IEEE Trans. Microwave Theory Tech., vol. MTT-43, pp. 2845-2849, Dec., 1995.
5. *Nefyodov E.I., Saidov A.S., Tagilaev A.R.* Wide-band microstrip controlling devices on microwave. - Moscow: Radio & Communication, -1994. (Rus.)
6. *Davidovitz M.* Wide-band waveguide-to-microstrip transmission and power divider // IEEE Trans. Microwave Theory Tech., vol. MTT-44, -№1, -1996. -pp. 13-15.
7. Physical principles of microwave and quasi-microwave volumerically integrated circuits / *Gvozdev V.I., Kuzaev G.A., Nefyodov E.I., Yashin A.A.* // Uspekhi Fizicheskikh Nauk, vol. 162, N3, Mar., 1992, -pp. 127-161. (Rus.)
8. *Bhat B., Koul S.K.* Analysis design and application of fin-line. - New York: Artech House, 1987.
9. *Neganov V.A., Nefyodov E.I., Yarovoy G.P.* The strip-slot structures on microwave and EHF. - Moscow: Science, 1996. (Rus.)
10. *Nefyodov E.I.* Open coaxial resonance structures (Review) // Radio Eng. & Electron. Phys., 1977, v.22, N9, pp. 1-28.
11. *Nefyodov E.I., Fialkovsky A.T.* Asymptotic theory of electromagnetic wave diffraction on limited bodies. -Moscow: Science, 1972.
12. *Nefyodov E.I., Sivov A.N.* Electrodynamics for periodic structures. -Moscow: Science, 1977.
13. *Kurushin E.P., Nefyodov E.I.* Electrodynamics of anisotropic waveguiding structures. - Moscow: Science, 1983.